Level structure of ^{60}Ni from the ^{58}Ni(α,2pγ) reaction

Tsan Ung Chan, C. Morand, F. Azgui, M. Agard,* J. F. Bruandet, B. Chambon,†
A. Dauchy, D. Drain,† A. Giorni, and F. Glasser
Institut des Sciences Nucléaires, 38026 Grenoble Cédex, France
(Received 25 May 1983)

The ^{60}Ni nucleus has been studied via the ^{58}Ni(α,2pγ) reaction at $E_\alpha=32$ MeV using in-beam γ spectroscopy techniques. High-spin states up to 10 MeV excitation have been established. Among the five branches depopulating the yrast $J^\pi=7^-$ state has been found an $E3$ transition down to the 4^+ state. Comparison with direct reaction results suggests the very likely $[\nu f_{5/2},\nu g_{9/2}]_{7-}$ configuration for the $J^\pi=7^-$ yrast state at 5349 keV, suggesting then the $[\nu(p_{1/2},p_{3/2},f_{5/2})^2_{2+}\times(\nu f_{5/2},\nu g_{9/2})^2_{7-}]_{9-}$ configuration for the $J^\pi=9^-$ yrast state. Other high-spin states might be accounted for by the breaking of the ^{56}Ni core.

[NUCLEAR REACTIONS ^{58}Ni(α,2pγ), $E=23-40$ MeV; measured E_γ, $I_{\gamma\gamma}(\theta)$, γ-γ coincidences, lifetimes by DSAM, ^{60}Ni deduced high-spin levels, J, π.]

I. INTRODUCTION

A large amount of experimental and theoretical work has already been devoted to the study of the ^{60}Ni nucleus. The experimental data till 1979 have been compiled by Auble.[1] In contrast with low-spin states ($J\leq 5$) where information is abundant, data on high-spin states ($J\geq 6$) are available only from gamma-ray spectroscopy. Ivanov *et al.*[2] and Moyat *et al.*[3] used heavy-ion induced reactions such as ^{46}Ti(^{16}O,2pγ), ^{50}Cr(^{12}C,2pγ), and ^{51}V(^{12}C,2npγ) to populate high-spin states in ^{60}Ni. An intense γ ray cascade, referred as a "*C*" cascade, has been observed with the yrast spin sequence: 0^+, 2^+, 4^+, 6^+, 7^-, 9^-. Recently Kearns *et al.*[4] used ^{56}Fe(^{7}Li,p 2nγ), ^{57}Fe(α,nγ), ^{56}Fe(^{6}Li,pnγ), and ^{52}Cr(^{10}B,pnγ) to get a more detailed scheme. In those reactions they observed the *C* cascade again, but no level above the 9^- state. Via direct reactions, Hansen *et al.*[5,6] have studied two-proton transfer with the ^{58}Fe(^{16}O,^{14}C)^{60}Ni reaction and α transfer with the ^{56}Fe(^{16}O,^{12}C)^{60}Ni reaction. Only levels up to $J^\pi=4^+$ have been excited in these reactions.

Theoretical studies concerning high-spin states are rather scarce. Ram Ray *et al.*[7] have calculated negative parity states up to the $J^\pi=7^-$ state at 5.30 MeV by means of the modified Tamm-Dancoff approximation and assuming a ^{56}Ni inert core and the four extra-core neutrons occupying the $p_{3/2}$, $f_{5/2}$, $p_{1/2}$, and $g_{9/2}$ single particle orbitals. The shell-model calculations of Koops *et al.*[8] kept the ^{56}Ni core but restricted the neutron orbitals to the $p_{3/2}$, $f_{5/2}$, and $p_{1/2}$ subshells so that they could only account for positive states up to $J^\pi=6^+$. Very recently, Potbhare *et al.*[9] extended the shell-model space to the ($p_{1/2}$,$p_{3/2}$,$f_{5/2}$,$g_{9/2}$) orbitals to explain the high-spin yrast cascade in this nuclei.

There is no doubt that the doubly magic nucleus ^{56}Ni with its first excited state $J^\pi=2^+$ at 2700 keV forms an utterly inert core, and coupled to the four-valence neutrons in the neighboring orbitals $p_{3/2}$, $f_{5/2}$, $p_{1/2}$, and $g_{9/2}$ (the single particle energies of which are, respectively, 0, 768, 1112, and 3710 keV in ^{57}Ni) it provides a powerful picture to describe most of the lowest levels in ^{60}Ni. With regard to the 3.7 MeV energy of the $g_{9/2}$ orbital, only one neutron may be $g_{9/2}$, thus giving negative parity states with, for example, the following configurations: $[g_{9/2},f_{5/2},(p_{3/2})^2_{0+}]_{7-}$, $[g_{9/2},f_{5/2},(p_{3/2},p_{1/2})^2_{2+}]_{9-}$, and $[g_{9/2},(f_{5/2})^2,p_{3/2}]_{10^-}$ and so $J^\pi\leq 10^-$.

For positive parity states this picture does allow the maximum spin $J^\pi\leq 6^+$ with configuration $[(f_{5/2})^2_{4+}$, $(p_{3/2})^2_{2+}]$, for instance. Higher spin states would require in the $g_{9/2}$ shell three neutrons for negative parity states and two neutrons for positive parity states. With regard to the large energy gap for the $g_{9/2}$ shell, the breaking of the ^{56}Ni core could be a cheaper way to build higher spin states. The α induced reaction used here surprisingly populates high spin levels in a better way than heavy-ion (HI) induced reactions, thus leading us to more detailed results.

II. EXPERIMENTAL PROCEDURE

Using beams from the Grenoble cyclotron, isotopic ~ 1 mg/cm^2 ^{58}Ni targets, and large volume Ge(Li) detectors (50–90 cm^3) with a typical resolution of 3 keV at $E_\gamma=1.3$ MeV, we have the following measurements: yield functions of γ rays at $E_\alpha=23-40$ MeV; angular distributions at $E_\alpha=32$ MeV; γ-γ coincidence at $E_\alpha=32$ MeV; lifetime measurements with the Doppler-shift attenuation method (DSAM) at $E_\alpha=32$ MeV; lifetime measurements by electronic methods (lower limit $\tau=3$ ns).

Figure 1 shows a single γ-ray spectrum of ^{58}Ni+α at $E_\alpha=32$ MeV. The main channels are (α,2pγ)^{60}Ni, (α,pnγ)^{60}Cu, and (α,αpγ)^{57}Co (the intensities are, respectively, in the 6:3:1 ratios). An accurate calibration of high energy gammas is provided by intense gamma rays from the radioactivity of ^{60}Cu (in particular, the following γ rays were used: 1332.5, 1791.6, 2158.9, and 3124.1 keV).

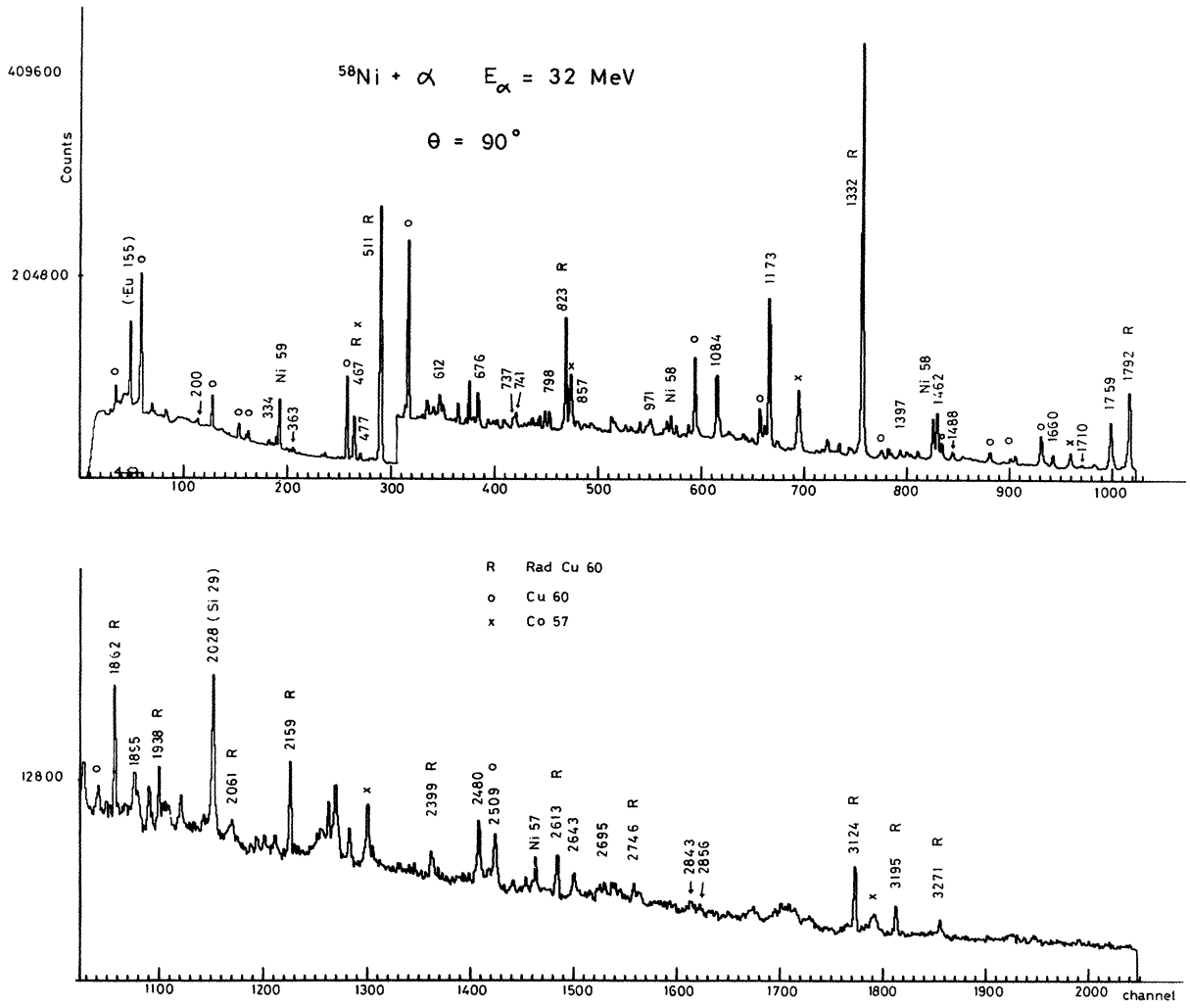

FIG. 1. Singles spectrum of the ^{58}Ni + α reaction at $E_\alpha = 32$ MeV.

III. ANALYSIS OF DATA

A. Yield functions

The yield functions were measured at 23, 27, 32, 36, and 40 MeV. Figure 2 shows the relative intensity of some γ rays. It may be noted that the 1660 keV γ depopulating a $J^\pi = 5^+$ state has a decreasing yield function because the 1173 keV γ ray intensity is mainly due to high-spin levels ($J^\pi \geq 7^-$).

B. Angular distributions

The angular distributions were performed at eight angles from 30° to 150°, on an isotopic target with Bi backing in order to reduce Doppler shifts. Results of the analysis are gathered in Table I. Formula and sign convention of Yamazaki[10] have been used.

Generally, it is not possible to obtain a unique spin assignment from this measurement alone. However, we quote only the final adopted solution with regard to the coherence of the whole available information. ($\gamma\gamma$ coincidences, yield functions, lifetimes measurements, and data from other reactions.) The arguments will be given in the discussion for each level. Several lines perturbed by radioactivity or by lines in other nuclei were not analyzed. The δ uncertainties were extracted from the χ^2 behavior in the vicinity of the minimum (the limits correspond to $1.4\chi^2$ minimum, which gives, even in the worst cases, a confidence level better than 80%). The alignment parameters were constrained to decrease from ~ 0.9 at the top of the yrast cascade to ~ 0.4 for the $J = 4$ level as has been shown by Taras and Haas.[11]

The adopted solution often corresponds to the one supported by a convergent set of weak proofs.[12]

C. $\gamma\gamma$ coincidences

An electronic timing measurement has shown no isomeric levels with $T_{1/2} > 2$ ns. Thus, prompt $\gamma\gamma$ coin-

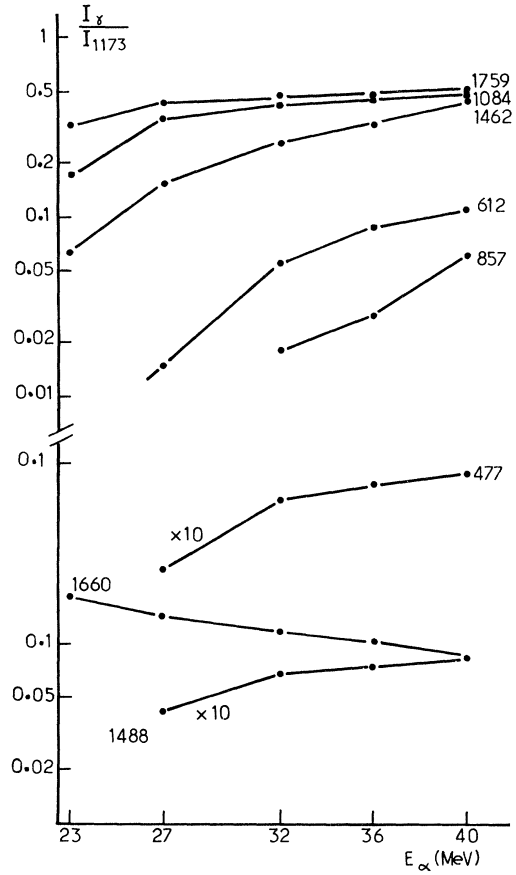

FIG. 2. Relative yield functions of some γ rays in ^{60}Ni.

cidences are sufficient to establish the level scheme. The data were recorded on magnetic tapes in the 2048×2048 format [E_γ up to 2 MeV with one Ge(Li) and up to 4 MeV with the other one]. The two Ge(Li) detectors were perpendicular to the beam axis. The angle between them was 90° and they were separated by a thick sheet of Pb: In this way, the 511-511 keV coincidence from β^+ decay of ^{60}Cu and the backscattering from one detector to the other were strongly reduced. Figures 3 and 4 present some selected spectra observed in coincidence with events in the indicated regions.

D. DSAM lifetime measurements

The DSAM explained at length elsewhere[13] provides lifetimes by fitting the line shapes in backward and forward angle spectra using the well known electronic stopping power $d\epsilon/d\rho=0.15\epsilon^{1/2}$ and an effective nuclear stopping power[13] $d\epsilon/d\rho=ax/\exp(x^2/2)$ with $x=b\epsilon^{1/2}$, ϵ being a reduced energy of the recoiling nucleus. The Doppler broadened peak shape is independent (χ^2 only changes less than 1%) of the apparent lifetime τ_a of the level provided that τ_a is longer than a limit $\tau_1\simeq 10$ ps because the Doppler shifted peak is then solely due to the part of the nuclei recoiling into the vacuum; the unshifted peak counts the nuclei stopped inside the target. Figure 5 shows a few examples of the fits obtained.

When neighboring lines completely perturbed the Doppler shifted peak and hence the lifetime measurements, we could sometimes obtain from γ spectra with a Bi-backed target limits on lifetimes from the following considerations. From a DSAM point of view, according to the value of the apparent lifetime τ_a of the level, prompt γ rays ($\tau_a<3$ ns) may have one of the two following asymptotical behaviors:

(i) "long lifetime" γ rays ($\tau_a>4$ ps) where the Doppler shift is mainly due to the emitting nuclei going out of the 0.9 mg/cm^2 target (this value $\tau_a=4$ ps is different from $\tau_1=10$ ps because it is the upper limit of reliable measurement range by means of DSAM). Because of the strong stopping power of Bi, the adding of Bi backing suppresses the Doppler shifted peak. So the unshifted peak remains alone in the spectrum whatever the detector angle is as can be seen in Fig. 6 for the 1084 keV γ ray in ^{60}Ni.

(ii) "short lifetime" γ rays ($\tau_a<0.6$ ps) for which the Doppler effect is essentially due to nuclei recoiling inside the target (this limit $\tau_a=0.6$ ps is the stopping time of a ^{60}Ni recoiling in ^{58}Ni with the initial velocity of the center of mass). The Bi backing has no effect in this case as can be seen in Fig. 6 for the 1224 keV γ ray in ^{57}Co for which $\tau=0.08$ ps and $\tau_a\simeq 0.6$ ps.

Therefore, when the Bi backing partly suppresses the Doppler-shifted peak, it means that τ_a lies in the range defined by the above assymptotical limits, i.e., $0.6<\tau_a<4$ ps. Table II presents the results of our measurements.

IV. SPIN-PARITY ASSIGNMENTS

Spin-parity assignments have been deduced with more or less reliance using the following: the fact that in the fusion evaporation reactions, γ cascades usually proceed from higher to lower spin; the angular distribution measurements (see Table I); the yield functions—increasing slope corresponds to increasing spin in a straight cascade; the lifetime measurements or estimations (see Table II); and the coherence of the established level scheme.

The deduced level scheme is shown in Fig. 7. Table III presents the branching ratios of some levels in ^{60}Ni. Because the lower states are well known, we only discuss levels with excitation energy higher than 4 MeV:

The 4165.2 keV level. The assignment $J^\pi=5^+$ of Barker *et al.*[14] is confirmed because of the undoubtedly $M1/E2$ character of the 1660 keV γ ray ($A_2=-1$ and $\delta=-1^{-0.4}_{+0.5}$ in agreement with Kearns *et al.*[4]). Our limits set on the lifetimes through DSAM $1.2<\tau<4$ ps is in the vicinity of their measurement 1.2 ± 0.6 ps for which they neglected the effects of contamination.

The 4264.9 keV level. It belongs to the so-called *C* yrast cascade and the assignment $J^\pi=6^+$ of Moyat *et al.*[3] and Kearns *et al.*[4] is obviously confirmed. There is also a weak branch of 4% which decays to the 4_2^+ state at 3120 keV through a 1145 keV transition.

The 4407.2 keV level. Three γ rays depopulate this weakly fed new state; none of them have reliable angular distributions. It may only be suggested from poor arguments (angular distribution, weak populating, and levels

TABLE I. Results of the angular distribution measurements. The E_γ transition decays from the E_i state ($J^\pi=J_i$) to E_f state ($J^\pi=J_f$). A_2 and A_4 are coefficients of Legendre polynomials from $I(\theta)=I_0[1+A_2P_2(\cos\theta)+A_4P_4(\cos\theta)]$ with $I_0(1173.2)=100$. The intensity of the 1173.2 keV γ lines is chosen for the normalization because the 1332.5 keV γ line has an important contribution from the radioactivity of ^{60}Cu. The alignment parameters α_2^i and α_2^f of the initial and final levels are computed using a Gaussian substate distribution of width α with formula and notations of Yamazaki (Ref. 10).

E_γ	$E_i\rightarrow E_f$	I_0	$A_2\pm\Delta A_2$	$A_4\pm\Delta A_4$	$J_i\rightarrow J_f$	σ	α_2^i	α_2^f	$\delta\pm\Delta\delta$	χ^2	Multipolarity and remarks
200.3	5348.8→5148.5	1.4	−0.44±0.09	−0.3 ±0.16	$7^-\rightarrow(6^-)$	2.25	0.73	0.70	$-0.17^{-0.5}_{+0.2}$	1.7	
242.0	4407.2→4165.2	1.5	−0.06±0.3	0.53±0.35	?→5						
334.0	5348.8→5014.8	6.1	0.19±0.07	−0.12±0.11	$7^-\rightarrow5^-$	2.3	0.72	0.66	$-0.1^{-0.15}_{+0.1}$	0.9	$E2$
362.9	5348.8→4985.9	3.1	−0.32±0.06	−0.02±0.09	$7^-\rightarrow6^+$	2.4	0.70	0.67	$-0.07^{-0.5}_{+0.3}$		$E1$
467.2	2626.0→2158.8				$3^+\rightarrow2^+$						Rad ^{60}Cu
476.8	8520.6→8043.8	5.3	−0.32±0.04	−0.10±0.06	(10)→(9)	2.5	0.83	0.82	$-0.03^{-0.10}_{+0.10}$	1.4	
498.0	3124.0→2626.0				$2^+\rightarrow3^+$						Rad ^{60}Cu
611.6	9132.2→8520.6	4.4	−0.45±0.08	−0.15±0.13	(11)→(10)	2.4	0.89	0.88	$-0.1^{-0.15}_{+0.15}$	1	
676.4	5662.3→4985.9				$(7^+)\rightarrow6^+$						Perturbed by γ in ^{57}Co
721.0	4985.9→4264.9	~2.2			$6^+\rightarrow6^+$						
737.0	4407.2→3670.2	~3.5			?→(4)						
741.3	5148.5→4407.2	~4			$(6^-)\rightarrow$?						
798.0	6460.3→5662.3	6.1			$8^+\rightarrow7^+$						Perturbed by γ in ^{59}Ni
857.3	9989.5→9132.2	4			?→(11)						
970.6	7430.9→6460.3				$?\rightarrow(8^+)$						
1083.9	5348.8→4264.9	30.5	−0.40±0.02	0.06±0.03	$7^-\rightarrow6^+$	2.1	0.77	0.74	$-0.1^{-0.3}_{+0.1}$	1.6	$E1$
1145.2	4264.9→3119.7				$6^+\rightarrow4^+$						
1184.5	3670.2→2505.7				$(4)\rightarrow4^+$						Perturbed by γ in ^{60}Cu
1173.2	2505.7→1332.5	100	0.18±0.05	−0.09±0.09	$4^+\rightarrow2^+$	2.0	0.48	0.34	$-0.09^{-0.3}_{+0.5}$	1	$E2$
1207.2	8043.8→6836.6	2	0.36±0.17	0.17±0.27							
1293.5	2626.0→1332.5				$3^+\rightarrow2^+$						Rad ^{60}Cu
1332.5	1332.5→0				$2^+\rightarrow0^+$						Important contribution from
1344.6	5014.8→3670.2	0.5			$5^-\rightarrow4^+$						Rad ^{60}Cu
1397.4	5662.3→4264.9	3.3	−0.63±0.14	0.28±0.17	$(7^+)\rightarrow6^+$	2.1	0.78	0.74	$-0.3^{-0.5}_{+0.2}$	1.1	$M1/E2$
1461.9	6810.7→5348.8	21.4	0.22±0.04	0.03±0.21	$9^-\rightarrow7^-$	2.5	0.79	0.76	$-0.1^{-0.15}_{+0.2}$	3	$E2$
1487.8	6836.6→5348.8	4.7	−0.11±0.12	0.2 ±0.16	$?\rightarrow7^-$						
1659.5	4165.2→2505.7	5.3	−1.0 ±0.1	0.43±0.09	$5^+\rightarrow4^+$	1.5	0.77	0.64	$-1^{-0.4}_{+0.5}$	2.1	$M1/E2$
1709.9	8520.6→6810.7	1.5			$?\rightarrow9^-$						
1759.2	4264.9→2505.7	45.0	0.21±0.04	−0.11±0.07	$6^+\rightarrow4^+$	2.7	0.54	0.48	$-0.1^{-0.2}_{+0.4}$	0.8	$E2$
1787.2	3119.7→1332.5	11	0.13±0.07	−0.05±0.12	$4^+\rightarrow2^+$	2.2	0.41	0.28	$-0.16^{-0.2}_{+0.5}$	0.8	$E2$
1791.5	3124.0→1332.5				$2^+\rightarrow2^+$						Rad ^{60}Cu
1895.1	5014.8→3119.7	2.4	−0.53±0.07	0.14±0.09	$5^-\rightarrow4^+$	1.9	0.64	0.58	$-0.18^{-0.2}_{+0.5}$	1.3	$E1$
1901.5	4407.2→2505.7	1	−0.04±0.3	0.2 ±0.3	$?\rightarrow4^+$						
2158.8	2158.8→0				$2^+\rightarrow0^+$						Rad ^{60}Cu
2480.2	4985.9→2505.7	8.7	0.30±0.08	−0.06±0.1	$6^+\rightarrow4^+$	2.4	0.6	0.53	$0^{-0.1}_{+0.3}$	0.9	$E2$
2509.2	5014.8→2505.7				$5\rightarrow4^+$						Perturbed by γ in ^{60}Cu
2642.8	5148.5→2505.7	2.9	0.34±0.11	−0.11±0.18	$(6^-)\rightarrow4^+$	1.9	0.74	0.66	$0^{-0.2}_{+0.3}$	0.8	
2695.0	8043.8→5348.8	2	0.4 ±0.3	−0.3 ±0.4							
2843.1	5348.8→2505.7	0.8	0.40±0.07	0.05±0.10	$7^-\rightarrow4^+$	2.7	0.62	0.52	$-0.15^{-0.20}_{+0.50}$	1	$E3$
3124.0	3124.0→0				$2^+\rightarrow0^+$						Rad ^{60}Cu

which feed or are fed by this state) that the spin may be (5,6).

The 4985.9 keV level. Recently reported by Kearns *et al.*[4] who suggested $J^\pi=(6^+)$ or (8^+), this state might be the 5050 keV ($J^\pi=6^+$) level seen via ^{60}Ni(e,e′) by Torizuka *et al.*[15] The 80% branch $E2$ transition (2480 keV, $A2=0.3$, $\tau=1.5^{-1}_{+3.5}$ ps) decaying to the $J^\pi=4^+$ yrast level wholly confirms $J^\pi=6^+$.

The 5014.8 keV level. This new level, not seen in heavy-ion induced or direct reactions decays to three 4^+ levels and perhaps to the 2^+ level at 2159 keV. The 1895 keV γ ray has an $L=1$ character. The 2509 keV transi-

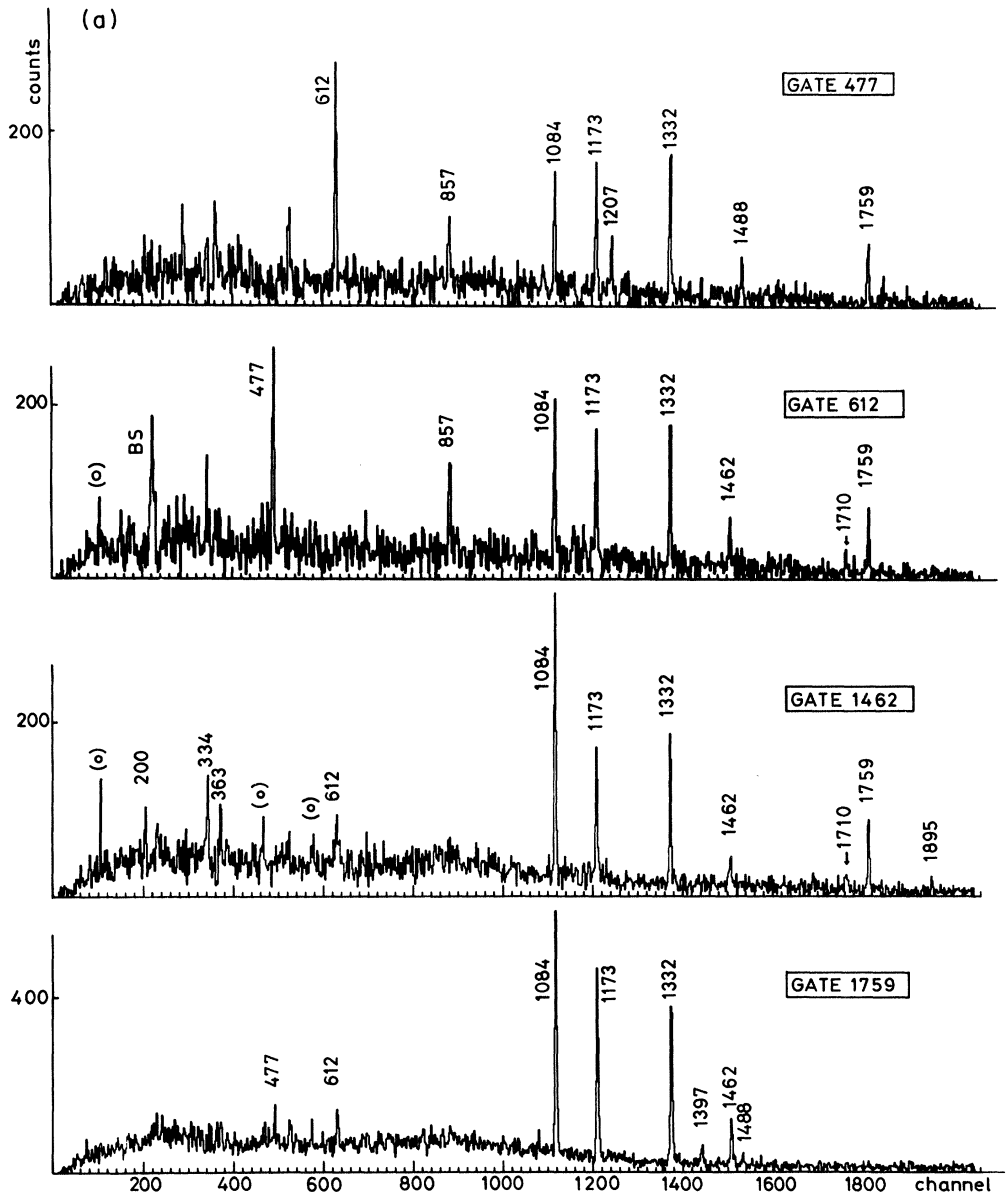

FIG. 3. (a) Selected spectra in coincidence with events in the indicated regions and with subtracted background. BS indicate back-scattering effects and (○) denote contamination from the ^{60}Cu 617 and 1469 keV γ rays in the 612 and 1462 gates. (b) Spectra in coincidence with gates corresponding to levels built on the 5^+ 4165 keV level.

tion to the 4^+ yrast state is perturbed by another γ ray of about the same energy in ^{60}Cu (Ref. 16). The 334 keV γ ray which depopulates the 7^- yrast state and which feeds the 5014 keV level has a clear enough $E2$ character ($A2=0.19$) to make sure of the $J^\pi=5^-$ assignment to this new level. The transition intensities deduced from its lifetime $\tau<4$ ps are usual for $E1$ transitions (see Table III) according to the recently compiled values in the 45–90 mass region by Endt.[17] The questionable $E3$ 2856 keV γ ray has not been clearly seen in coincidence with the 334 keV gate, but this gate shows a line at 826 keV which is also present in prompt spectra with a much greater intensity than it should be for a pure ^{60}Cu radioactivity line (the 467 keV is missing).

The 5148.5 keV level. This new level decays through two γ rays. The 2643 keV line likely has the $L=2$ character ($A2=0.34\pm0.11$). The long lifetime (4 ps $<\tau<$ 3 ns) would exclude the $E2$ character and thus give $J^\pi=(6^-)$ to this level. This assignment is supported by the probable $M1/E2$ character of the 200 keV transition which feeds this level from the $J^\pi=7^-$ yrast level.

The 5348.8 keV level. From this work, nothing can be added to the characteristics of this well known yrast $J^\pi=7^-$ state. Polarizations by Moyat *et al.*[3] and RDM

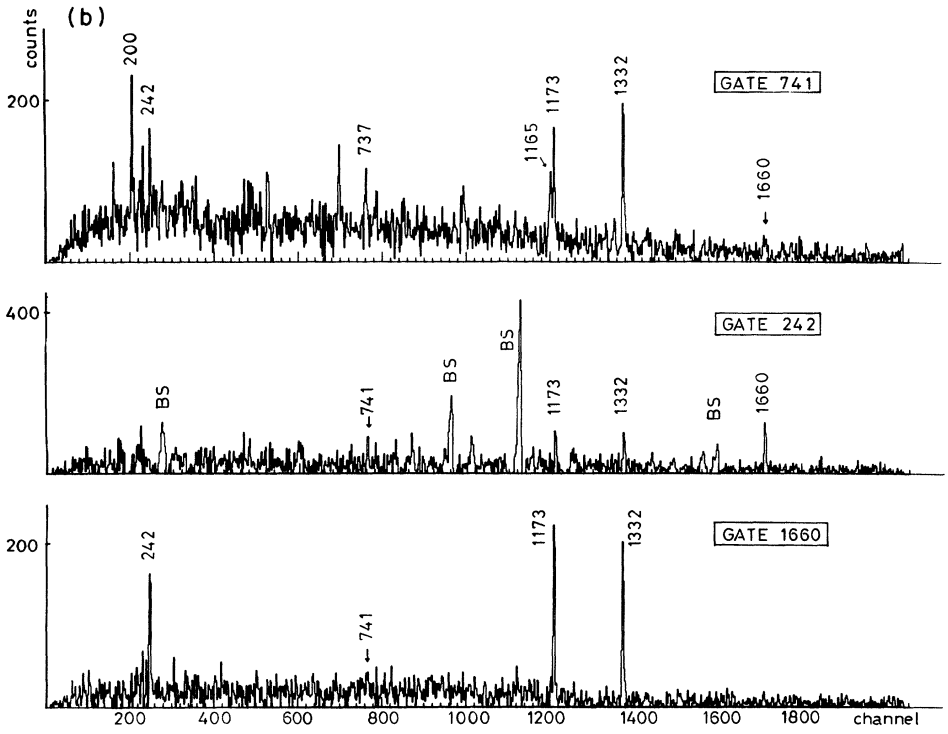

FIG. 3. (*Continued.*)

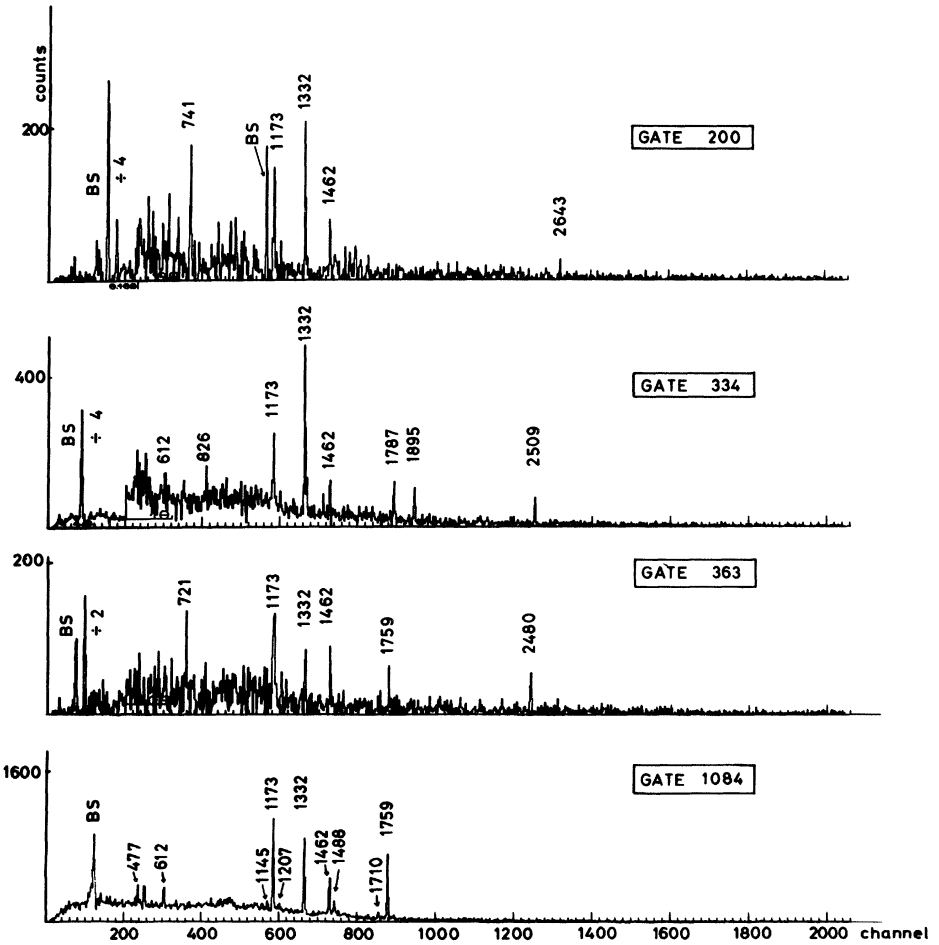

FIG. 4. Spectra in coincidence with gates corresponding to different branches of the 7^- state at 5348.8 keV.

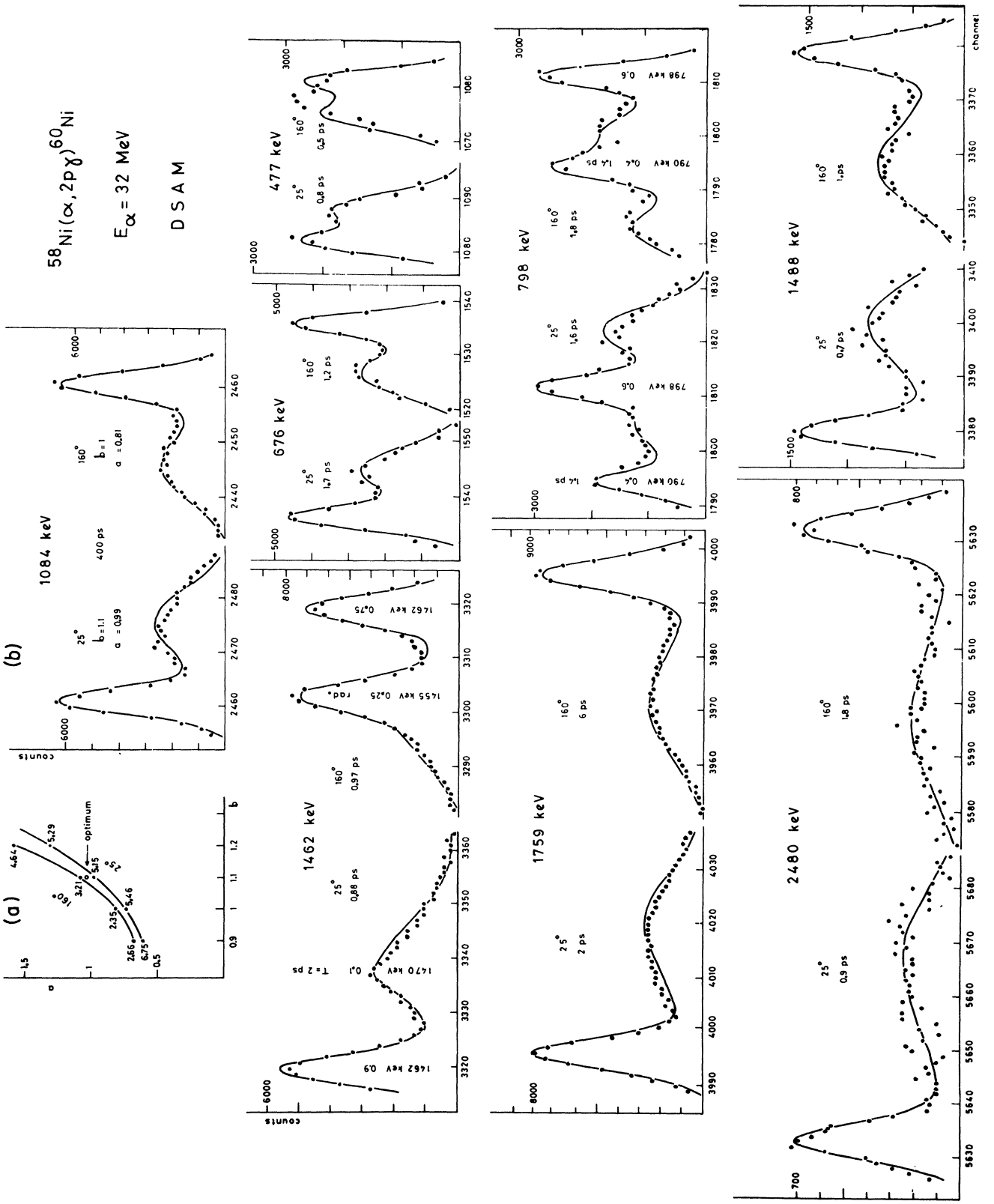
58Ni(α,2pγ)60Ni
Eα = 32 MeV
DSAM
(a)
(b)
1084 keV
400 ps
1462 keV
1759 keV
798 keV
2480 keV
1488 keV
676 keV
477 keV
counts
channel

TABLE II. Lifetimes measurements of ^{60}Ni levels. The measured lifetime level has E_x (keV) excitation energy and characteristics J^π. The Doppler distorted γ ray of E_γ (keV) issued from this level gives at θ_m° the measured lifetime value τ_m; τ_f is the adopted final value averaging the various τ_m according to confidence considerations such as lower χ^2 fit and neatness of the peak. (In the inequalities τ_m and τ_f is the central value flanked by the lower τ_l and upper τ_u limits of the measurements.) $|M|^2$ is the deduced Weisskopf intensity of the transition E_γ. τ are given in ps. The remarks indicate whether the γ ray has been fitted at the same time as a neighboring one (see Fig. 5). The asterisks denote the cases where one of the limits was extracted from the comparison between Doppler behaviors in spectra performed with either self-supporting or Bi backed targets (see Fig. 6). + indicates the electronic limit $\tau < 3$ ns.

						$\lvert M\rvert^2$ in W.u.			
E_x	J^π	E_γ	θ_m°	$\tau_l < \tau_m < \tau_u$	$\tau_l < \tau_f < \tau_u$	$E1$	$M1$	$E2$	Remarks
3120	4^+	1787			0.35 ± 0.15[a]			9	
4165	5^+	1660	25	$1.4 < \tau_m$	$1.2 < 2 < 4^*$		1.7×10^{-3}	1.1	
			160	$1 < \tau_m$					
4265	6^+	1759	25	$0.5 < 2 < \infty$	0.7 ± 0.4[a]			1.1	
			160	$1 < 6 < \infty$					
4407		737	25	$2 < 4 < \infty$	$4^* < \tau_f < 3000^+$	$<2.4\times10^{-4}$	$<1.2\times10^{-2}$	<40	mixed with the 741 keV γ ray
			160	$0 < 2 < 10$					
4986	6^+	721	25	$0.4 < 1 < 15$	$0.5 < 1.5 < 5$		5.6×10^{-2}		
			160	$0 < 1.7 < 10$					
		2480	25	$0.4 < 0.9 < 3$				0.3	
			160	$0.6 < 1.8 < 10$					
5015	5^-	1895	160	$0.06 < 0.25 < 1.5$	$0.1 < 0.3 < 4$	$>1.2\times10^{-5}$			mixed with γ
		2509	25	$0.14 < 0.5 < 6$					of the same energy
			160	$0.1 < 0.3 < 5$		$>0.35\times10^{-5}$			in ^{60}Cu
5146	(6^-)	2643	25	$0.5 < 2 < \infty$	$4^* < \tau_f < 3000^+$			$<4.5\times10^{-2}$	
			160	$1 < \tau_m$					
5662	(7^+)	676	25	$0.6 < 1.7 < 7$	$0.6 < 1 < 4^*$	1.2×10^{-3}	6.2×10^{-2}	250	
			160	$0.7 < 1 < 3$					
		1397	25	$0.14 < 0.7 < 8$		8×10^{-5}	4×10^{-3}	4	doubtful
			160	$0.2 < 1 < 8$					mixing ratio
6460	(8^+)	798	25	$1 < 1.65 < 4$	$1 < 1.7 < 4$	7.4×10^{-4}	3.7×10^{-2}	110	
			160	$1.1 < 1.8 < 4$					mixed with
6811	9^-	1462	25	$0.66 < 0.88 < 1.3$	$0.6 < 0.9 < 1.5$			10	1469 keV
			160	$0.66 < 0.97 < 2$					mixed with
									1454 keV
6837	(8)	1488	25	$0.5 < 0.67 < 0.9$	$0.5 < 0.8 < 1.5$	2.4×10^{-4}	1.2×10^{-2}	10	
			160	$0.6 < 1 < 2$					
8044	(9)	1207	25	$0.05 < 0.5 < 2$	$0 < 0.05 < 0.5$	3.6×10^{-5}	0.18	230	very weak at
		2695	25	$0 < 0.02 < 0.4$		3.2×10^{-4}	1.6×10^{-2}	4	forward and
			160	$0 < 0.02 < 0.3$					backward
									angles
8521	(10)	477	25	$0.5 < 0.8 < 1.5$	$0.4 < 0.7 < 1.5$	6.7×10^{-3}	0.33	2700	
			160	$0.25 < 0.5 < 1.5$					
9132	(11)	612	25	$0.24 < 0.33 < 0.4$	$0.15 < 0.26 < 0.4$	1.1×10^{-2}	0.53	2600	mixed with
			160	$0.1 < 0.2 < 0.4$					617 keV of
									^{60}Cu
9990	(12)	857	25	$0.15 < 0.26 < 0.4$	$0.2 < 0.3 < 0.6^*$	3.4×10^{-3}	0.17	420	
			160	$0.24 < 0.4 < 0.8$					

[a]From Kearn's work[4] and consistent with present measurements.

FIG. 5. Line shape fits for lifetime measurements by DSAM. The top row displays the extraction of nuclear stopping power parameters for DSAM. At forward ($\theta=25°$) and backward ($\theta=160°$) angles, the 1084 keV line has been fitted for different nuclear stopping powers parameters ($b=0.9$, 1.0, 1.1, 1.2; a in the 0.5—2.0 range). (a) gives the corresponding two χ^2 valleys in the a vs b plane, with the χ^2 minimum numerical values. The selected nuclear stopping power indicated by a circle arrowed as the optimum has $b=1.1$ and $a=1.08\pm0.05$, the incertitude has been deduced from the gap between the two curves. (b) gives the lowest χ^2 minimum fit at each angle. The bottom rows displays the lowest χ^2 fits which illustrate lifetime measurements using the above extracted stopping power as well for a well-shaped line (1759 keV) as for a bad-shaped line (477 keV) due to statistics. Two of them have been fitted mixed with a neighboring line of known lifetime; the energy, the relative intensity, and the lifetime of the perturbing line are written vertically at the full energy channel.

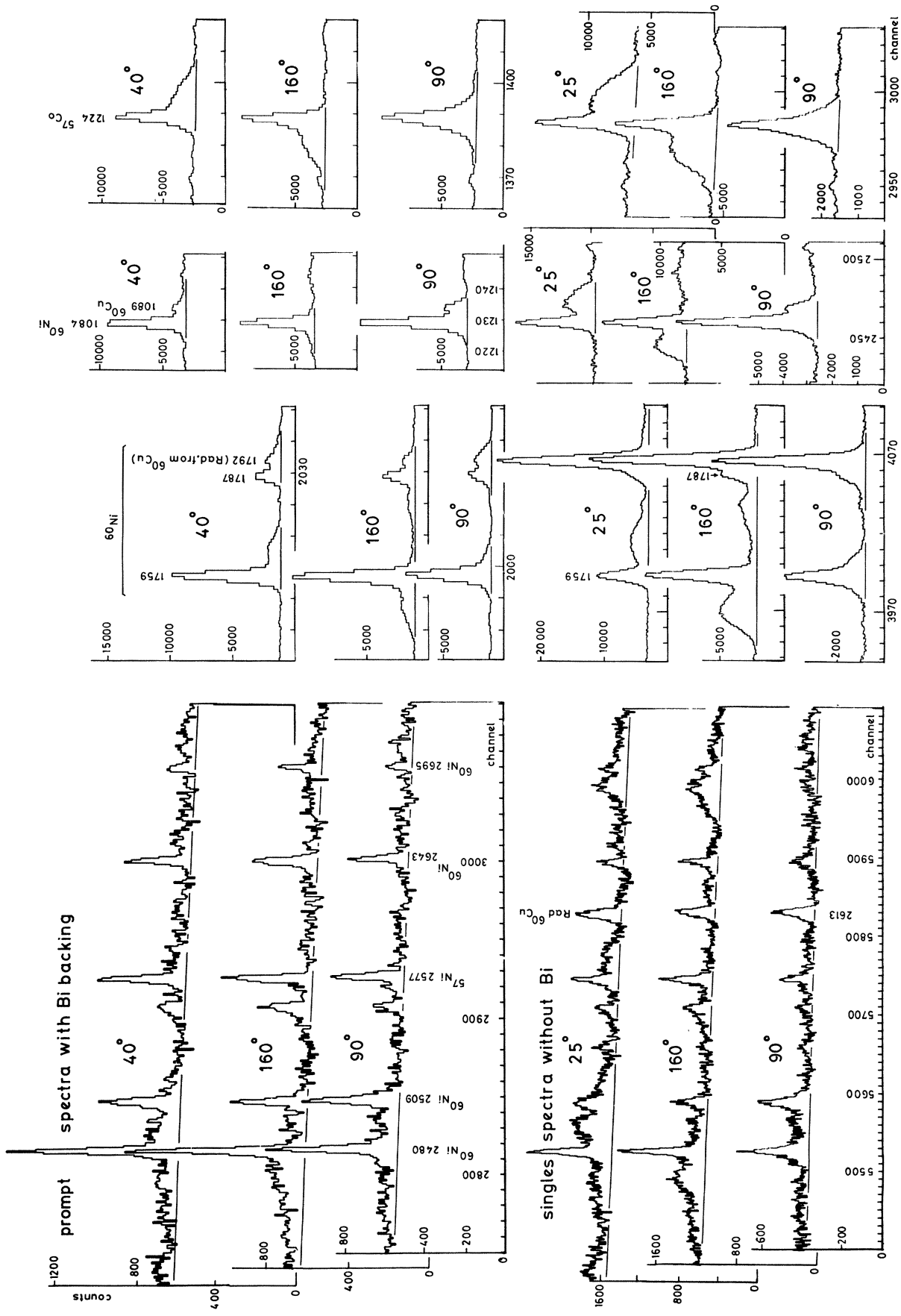

FIG. 6. The top spectra obtained with a Bi backed target are prompt spectra (i.e., recorded at the same time as the beam bursts arrival on the target, which explains the absence of radioactivity). The bottom singles spectra have been obtained with a self-supporting target of ^{58}Ni. Comparison between them provides lifetime information.

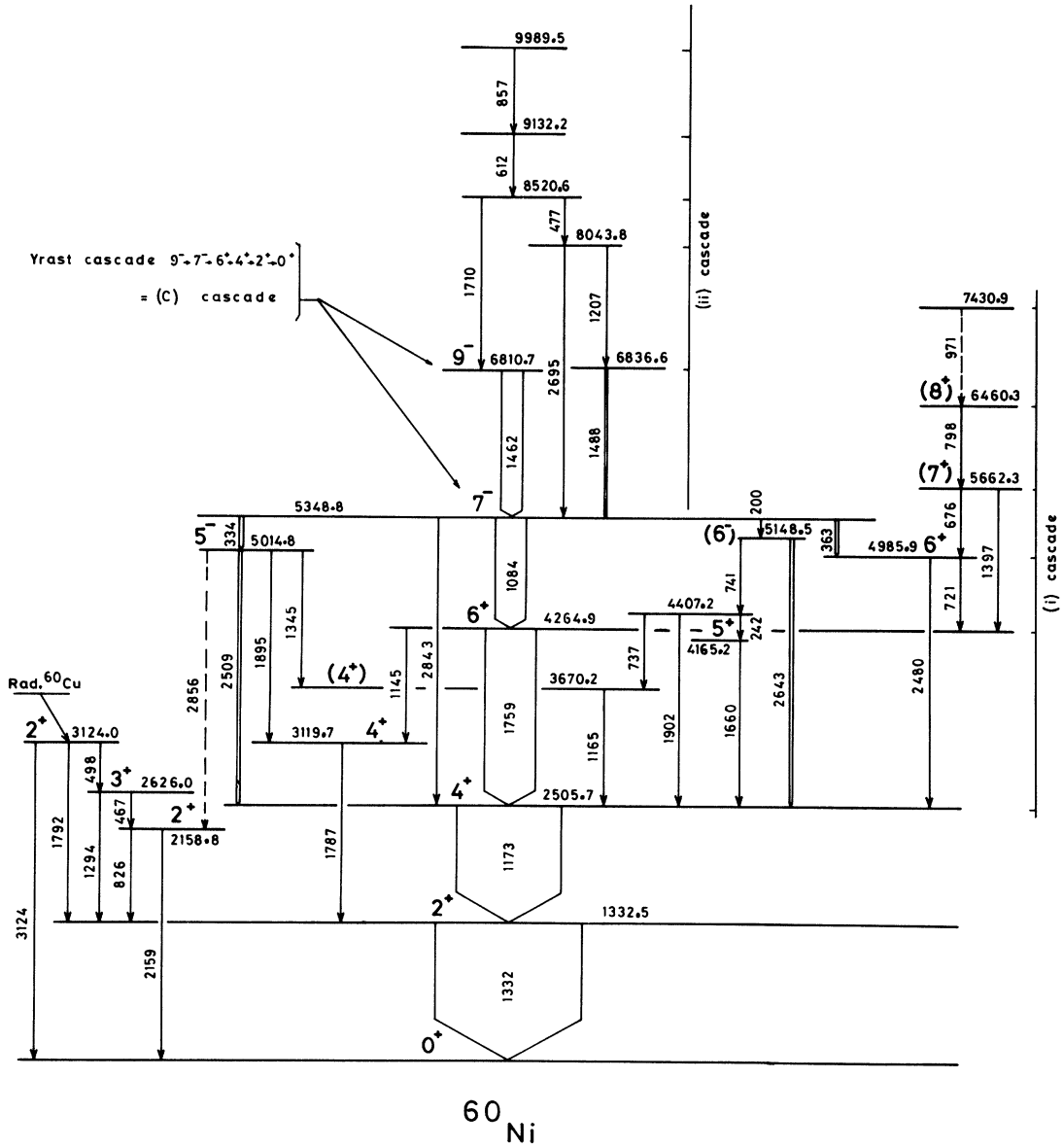

FIG. 7. Decay scheme of ^{60}Ni as a result of the present measurements. The C yrast (i) and (ii) cascades are indicated to make the discussion clearer.

lifetime by Moyat *et al.*[3] and Kearns *et al.*[4] have utterly ruled out the $J^\pi=7^+$ characteristics suggested by Ivanov *et al.*[2] However, we established that this long lived state decays in five distinctive ways (two of them are known so far[4]). One branch is a 2843 keV $E3$ transition to the $J^\pi=4^+$ yrast state (see Table III); its angular distribution has an $E3$ transition behavior ($A_2 \gg 0$ and $A_4 \gtrsim 0$; see Table I). This $J^\pi=7^-$ level might be identified as the most strongly excited state seen at 5.53 ± 0.10 MeV by Van Driel *et al.*[18] via (α,^{2}He) and at 5.4 MeV by Ost *et al.*[19] via the (^{13}C,^{11}C) reaction.

The 5662.3 keV state. We confirm the existence of this level already seen by Kearns *et al.*[4] The characteristics of $J^\pi=(7^+)$ are quasicertain with regard to the $M1/E2$ 1397 keV transition ($A2=-0.6$, $\delta=-0.3$). We add another branching of 60%: 676 keV to the 6^+ state at 4986 keV; unfortunately, perturbed by a γ ray in ^{57}Co. The measured $\tau=1^{-0.4}_{+3}$ ps lifetime of this level gives a transition intensity which only excludes $J=8$ but does not allow a choice between $E1$ and $M1$ (see Table II).

The 6460.3 keV state. The 798 keV γ ray is perturbed by a line belonging to the ^{59}Ni and no spin assignment can be deduced. However, Kearns *et al.*[4] saw this line on the 721 keV gate (which is correct) and thus built a level 798 keV above the 4986 keV state (which is wrong because the 798 keV is also seen in coincidence with the 676 and 1397 keV lines). They found that the 798 keV γ ray has an $M1$ character, which would assign $J^\pi=(8^+)$ to this new level.

The 6810.7 keV state. Our results thoroughly confirm the characteristics $J^\pi=9^-$ assigned by Moyat *et al.*[3] and Kearns *et al.*[4] to this level which was the last one of the C cascade that they saw in heavy-ion reactions. Only one

TABLE III. Branching ratios in ^{60}Ni. The remarks indicate where intensities could not have been straightly extracted from angular distribution analysis, but were estimated from coincidence spectra. Otherwise, errors on the BR are of 10%.

E_i	J_i^π	E_f	J_f^π	E_γ	BR	Remarks
4265	6^+	3120	4^+	1145	4	
		2506	4^+	1759	96	
4407	(5,6)	4165	5^+	242	20	
		3670	(4)	738	60	
		2506	4^+	1902	20	
4986	6^+	4265	6^+	721	20	
		2506	4^+	2480	80	
5015	5^-	3670	(4^+)	1345	10	gate 334 keV
		3120	4^+	1895	54	
		2506	4^+	2509[a]	35	
		2159	2^+	2854	1	
5148	(6^-)	4407	(5,6)	741	60	error 30% on BR
		2506	4^+	2643	40	
5349	7^-	5148	(6^-)	200	3	
		5015	5^-	334	17	
		4986	6^+	363	8	
		4265	6^+	1084	70	
		2506	4^+	2843	2	
5662	(7^+)	4986	6^+	676[b]	60	gate 798 keV
		4265	6^+	1397	40	
8044	(9)	6837	(8)	1207	50	error 30% on BR
		5349	7^-	2695	50	
8521	(10)	8044	(9)	477	80	
		6811	9^-	1710	20	

[a]Perturbed by a line in ^{60}Cu.
[b]Perturbed by a line in ^{57}Co.

discrete weak line quaintly appears to feed this strongly populated state.

The 6836.6 keV state. The $L=1$ character of the 1488 keV γ transition depopulating this new level cannot be positively established from angular distribution analysis. The increasing of its yield function suggests $J=(8)$ but the Weisskopf estimate ($|M|^2=10$) of the 1488 keV transition, if it were $E2$, cannot exclude $J=9$.

The 8043.8 keV state. This new level decays via two weak γ rays. The angular distributions analysis seems to lead to conflicting results with both $L=2$ ($A2>0$) transitions. The $J=9$ suggestion may be supported by the increasing slope of the yield curve and would give a correct Weisskopf estimate of the 2695 keV γ ray intensity if it were $E2$ (and thus gives negative parity to the level).

The 8520.6 keV state. No reliable information can be extracted from the 1710 keV γ ray leading to the $J^\pi=9^-$ yrast state. However, the angular distribution of the 477 keV clearly gives $L=1$, and its lifetime excludes the $E2$ character so that the spin of the 8520.6 keV state would be $J=10$ if the 8043.8 keV state were $J=9$.

The 9132.2 keV state. The angular distribution of the 612 keV γ ray suggests an $L=1$ ($M1/E2$?) transition, and the lifetime limits also exclude the $E2$ character. The rapidly increasing yield function therefore suggests $J=(11)$.

The 9989.5 keV state. This latest top level reached via the (α,2pγ) reaction beyond the proton emission threshold ($E_p\sim 9.5$ MeV) decays through a 857 keV line without reliable angular distribution. Yet the $E2$ character may be ruled out with regard to the $|M|^2=420$ corresponding intensity unacceptable for such high spin levels in quasi-spherical nuclei.

To conclude, the spin of the 8044, 8521, 9132, and 9990 keV levels is either 10, 11, 12, 13 or 9, 10, 11, 12 with a preference for the second choice.

V. CONCLUSION

A. Experimental results

The experimental results present two striking features:

(1) The 5348.8 keV $J^\pi=7^-$ level has indeed five branching transitions among which is a 2843 keV $E3$ transition connecting two high-spin states. The $|M|^2=0.3\pm0.03$ W.u. of this transition lies in the average of the values of $E3$ in the 45–90 masses given by Endt.[17]

TABLE IV. Comparison between shell model calculations[a] and experimental results for 5^+ and 6^+ states.

	Excitation energies (MeV)				Decay properties $\|M\|^2$ W.u.					
					$M1$			$E2$		
J_i	exp	MSDI	ASDI	J_f^π	exp	MSDI	ASDI	exp	MSDI	ASDI
5^+	4.165	4.03	3.36	4_1^+	$1.7^{-0.8}_{+1.1}\times10^{-3}$	4.6×10^{-3}	2.2×10^{-3}	$1.1^{-0.5}_{+0.7}$	8.3	6.1
				3^+	b			b	5.9	5.2
	(4.407)	4.39	4.39							
6^+	4.265	3.92	3.93	4_1^+	0			$1.1^{-0.4}_{+1.5}$	3.4	1.2
	4.986	4.95	4.56							

[a]Koops *et al.* (Ref. 8).
[b]Not seen experimentally.

(2) The yrast levels at 5349 and 6811 keV collect 42% and 21% of the total γ intensity which feeds the 4_1^+ state, while neighboring levels are very poorly populated. This may be noticed particularly about the following two cascades: (i) 4986-keV-6^+ — 5662-keV-(7^+) — 6460-keV-(8^+) — 7431-keV-(9^+); (ii) 8044-keV-(9) — 8521-keV-(10) — 9132-keV-(11) — 9990-keV-(12).

This strong difference of the intensities feeding those cascades and the $J^\pi=7^-$ and 9^- yrast levels is insufficiently accounted for by the poor supply of high angular momentum from α induced reactions, but must have a structure explanation. We suggest that the loss of intensity corresponds to a change of seniority (seniority 2 for 7^-, seniority 4 for 9^- with ^{56}Ni inert core) or the breaking of ^{56}Ni [the (i) and (ii) cascades might correspond to a seniority of 4 with the broken ^{56}Ni core].

B. Tentative theoretical interpretation

1. $J^\pi \leq 6^+$ states

For positive parity states with $J^\pi \leq 4^+$ the shell model calculations of Koops *et al.*[8] have given nice agreement with experiment for excitation energies as well as for electromagnetic properties although they restrict the configuration space of the four extra-core neutrons to the $2p_{3/2}$, $1f_{5/2}$, and $2p_{1/2}$ orbits surrounding the ^{56}Ni inert core. In this way they also account for the $J^\pi=5^+$ and 6^+ states. (See Table IV.)

2. $J^\pi=5^-$, (6^-), 7^-, 9^- states

Many arguments confirm the interpretation of the yrast 7^- and 9^- states as members of a rotational aligned

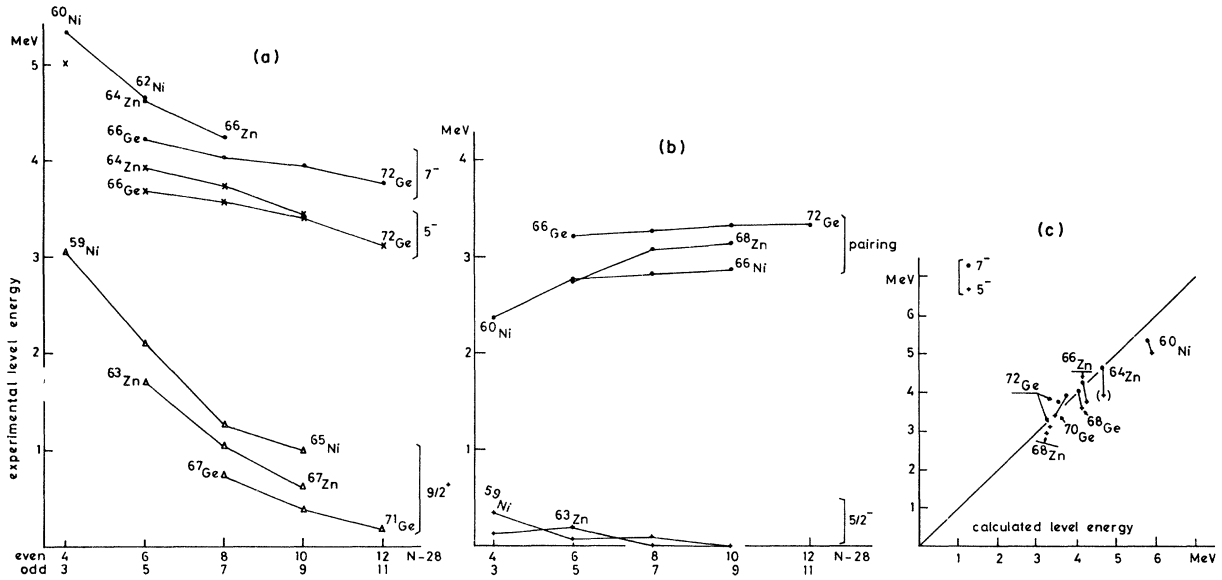

FIG. 8. The evolution of the $J^\pi=5^-$ and 7^- states energies through the Ni, Zn, and Ge isotopes when they are interpreted with $[(p_{3/2},f_{5/2})_{0^+}\times(p_{1/2},g_{9/2})^2_{5^-}]_{5^-}$ and $[(p_{3/2},p_{1/2})_{0^+}\times(f_{5/2},g_{9/2})^2_{7^-}]_{7^-}$ configurations. In (a) and (b) the abscissa represents $N-28$, where N is the neutron number of the even-even or even-odd nuclei. Top (a) displays a rather smooth evolution of the excitation energy, with a slightly smoother slope than the single particle neutron $g_{9/2}$ energy [low (a)]. This difference of slopes may be accounted for by the slightly increasing pairing energy and the weaker decreasing slope of the single particle neutron $f_{5/2}$ energy [top and low (b), respectively]. In (c) the abscissa represents the excitation energy calculated by means of our crude shell model (Ref. 20) which agrees very well with experimental results except for the ^{60}Ni case where the discrepancy reaches 10% for the $J^\pi=5^-$ level. In this model the energy of a two-nucleon configuration state is calculated as the addition of the single particle state energies taken from the neighboring nuclei plus the pairing energy if necessary.

negative-parity band formed by coupling a $g_{9/2}$ and an $f_{5/2}$ neutron to the core. In this mass region far from well deformed nuclei able to bring high spin collective states, the cheapest way to build negative parity states in the shell model framework is to call for the positive $g_{9/2}$ subshell at 3.7 MeV excitation in ^{57}Ni. Recently, via the two neutron transfer reaction ^{58}Ni(α,^{2}He)^{60}Ni, Van Driel *et al.*[18] clearly established the two-neutron configuration of a state at 5.52 MeV. Indeed, such a direct reaction at $E_\alpha = 65$ MeV is known to strongly select states for which both nucleons couple their spin at maximum. Van Driel *et al.*[18] performed DWBA calculations and found that the 5.52, 8.92, 9.80, and 10.85 MeV states angular distributions agree with an $L = 8$ transfer. However, they would also be compatible with $J^\pi = 7^-$ characteristics.

A two-neutron high-spin state has also been strongly selected at 5.4 MeV by Ost *et al.*[19] via the (^{13}C,^{11}C) reaction at $E_{^{13}C} = 105$ MeV. In order to confirm that the above $J^\pi = 5^-$ and 7^- states have $[p_{1/2},g_{9/2}]_{5^-}$ and $[f_{5/2},g_{9/2}]_{7^-}$ configurations it is interesting to follow the energy evolution of these states through the Ni, Zn, and Ge isotopes in Fig. 8(a). With an increasing number of neutrons, their excitation energy curve has a weaker slope than the $g_{9/2}$ single particle energy curve in the corresponding element, which is well explained by a slightly increasing pairing energy [Fig. 8(b)]. In the absence of shell-model calculations including the $g_{9/2}$ orbit, we have proposed a crude shell-model in order to account for two-nucleon high-spin states through the $Z = 28-32$ range.[20] The agreement between experimental and calculated values of excitation energies is illustrated in Fig. 8(c).

In order to argue about the sudden appearing of the $g_{9/2}$ neutrons in these 5^-, (6^-), 7^- states near 5 MeV, we may at last consider the hindrance of the transition rates to lower levels. Among the five branchings of the 7^- states, the $E2$ value of 6 W.u. to the 5^- level and the probable $M1$ value of 3.4×10^{-4} W.u. to the (6^-) level are right in the averages over the $A = 45-90$ nuclei according to Endt.[17] But the hindrances of the $E1$ transitions to levels which are not assumed to involve the $g_{9/2}$ orbital are found to be very strong: 3×10^{-6} and 10^{-6} W.u. which confirms a change of configuration.

The last strongly populated level, i.e., the 9^- yrast top state of the C cascade, is likely to have a configuration which involves $g_{9/2}$ neutrons with probably the $[g_{9/2},f_{5/2},(f_{5/2},p_{3/2},p_{1/2})_{2^+}]_{9^-}$ configuration since it appears to be strongly connected with the 7^- yrast state which is $[g_{9/2},f_{5/2},(f_{5/2},p_{3/2},p_{1/2})^2_{0^+}]_{7^-}$ by an $E2$ transition of 10 W.u.

3. *Tentative $f^{-1}_{7/2}$ neutron holes cascades*

The poor feeding of the (i) and (ii) cascades could be qualitatively explained in the framework of the above shell-model with four neutrons in the $p_{1/2}$, $p_{3/2}$, $f_{5/2}$, $g_{9/2}$ orbitals surrounding a ^{56}Ni core. Core excitations are possible since the 2.7 MeV energy of the first $J^\pi = 2^+$ excited state in ^{56}Ni is lower than the 3.7 MeV single particle $g_{9/2}$ orbital in ^{57}Ni. Such 2.7 MeV energy jumps happen in the ^{60}Ni level scheme at the bottom of the (i) and (ii) cascades with the 2.48 MeV and the 2.695 MeV intervals, respectively.

For the (i) cascade the $6^+\rightarrow4^+$ $E2$ transition has an intensity of $0.3^{-0.2}_{+0.6}$ W.u. which may be compared to the 6 W.u. of the $2^+\rightarrow0^+$ $E2$ γ ray in ^{56}Ni. The main configuration of the 2^+ state in ^{56}Ni is probably $(p_{3/2},f^{-1}_{7/2})_{2^+}$ and using the likely $(f_{5/2})^2_{4^+}$ configuration of the 4^+ yrast state in ^{60}Ni the above picture allows one to build the states

$$[(f_{5/2})^2_{4^+}\times(p_{3/2},f^{-1}_{7/2})_{2^+,3^+,4^+,5^+}]_{6^+,7^+,8^+,9^+}$$

at 4.98, 5.66, 6.46, and 7.43 MeV, respectively. Such a picture would agree nicely with rates of pure $M1$ transitions connecting the levels of the (i) cascade when angular distribution analysis and transition rates (Tables I and II) are considered.

A similar attempt may be done to interpret the (ii) cascade states also with configurations containing holes in the $f_{7/2}$ orbital. These configurations would be

$$[(g_{9/2},f_{5/2})_{7^-}\times(p_{3/2},f^{-1}_{7/2})_{2^+,3^+,4^+,5^+}]_{9^-,10^-,11^-,12^-}\,.$$

This tentative interpretation is supported by the experimental evidence of $(f^{-1}_{7/2}g_{9/2})$ levels in the 5–12 MeV excitation range from the result of Chang *et al.*[21] obtained via (α,t) and (α,^{3}He) on ^{59}Co at $E_\alpha = 120$ MeV and from electron scattering of Lindgren *et al.*[22]

---

*Permanent address: Institut des Sciences Exactes, Université de Constantine, Route d'Ain El Bey, Constantine, Algérie.

†Permanent address: Institut de Physique Nucléaire, UCB Lyon, IN2P3, 43 Bd du 11 Novembre 69261 Villeurbanne, France.

[1]R. L. Auble, Nucl. Data Sheets 28, 103 (1979).

[2]M. A. Ivanov, I. Kh. Lemberg, A. S. Meshin, I. K. Pecker, and I. N. Chuganov, Izv. Akad. Nauk. SSSR Ser. Fiz. 39, 1695 (1975) [Bull. Acad. Sci. USSR, Phys. Ser. 39, 108 (1975)].

[3]G. Moyat, B. Delaunay, J. Delaunay, J. Eberth, V. Zobel, and L. Cleeman, Nucl. Phys. A318, 236 (1979).

[4]F. Kearns, L. P. Ekstrom, G. D. Gones, T. P. Morisson, O. M. Mustaffa, H. G. Price, D. N. Simister, P. J. Twin, R. Wadsworth, and N. J. Ward, J. Phys. G 6, 1131 (1980).

[5]D. L. Hansen, Nelson Stein, J. W. Sunier, G. W. Woods, and Ole Hansen, Nucl. Phys. A321, 472 (1979).

[6]D. L. Hansen, Nelson Stein, G. W. Woods, J. W. Sunier, Ole Hansen, and B. S. Nilson, Nucl. Phys. A336, 290 (1980).

[7]Ram Ray, B. B. Roy, D. P. Rustgi, and M. L. Rustgi, Lett. Nuovo Cimento 23, 12 (1978).

[8]J. E. Koops and P. W. Glaudemans, Z Phys. A 280, 181 (1977); J. E. Koops, Thesis, Utrecht, 1978 (unpublished).

[9]V. Potbhare, S. K. Sharma, and S. P. Pandya, Phys. Rev C 24, 2355 (1981).

[10]T. Yamazaki, Nucl. Data Sect. A 3, 1 (1967).

[11]P. Taras and B. Haas, Nucl. Instrum. Methods 123, 73 (1975).

[12]H. Morinaga, Proceedings of the Conference on Present and Future Aspects of In Beam γ-ray Spectroscopy, Commissariat á l'energie Atomique, Aussois, 1978 (unpublished).

[13]C. Morand and Tsan Ung Chan, Comp. Phys. Com. 23, 393 (1981); C. Morand, J. F. Bruandet, B. Chambon, A. Dauchy, D. Drain, A. Giorni, and Tsan Ung Chan, Nucl. Phys. A313, 45 (1979).

[14]J. H. Barker and D. G. Sarantities, Phys. Rev. C 9, 607 (1974).

[15]Y. Torizuka, Y. Kojima, M. Oyamada, K. Nakakara, K. Sujiyama, T. Terasawa, K. Itok, A. Yamagushi, and M. Kimura, Phys. Rev. 185, 1499 (1969).

[16]Tsan Ung Chan, M. Agard, J. F. Bruandet, B. Chambon, A. Dauchy, D. Drain, A. Giorni, F. Glasser, and C. Morand, Phys. Rev. C 26, 424 (1982).

[17]P. M. Endt, At. Nucl. Data Tables 23, 547 (1979).

[18]J. Van Driel, R. Kamermans, R. J. De Meijer, and H. P. Marsch, Nucl. Phys. A350, 109 (1980); University of Groningen Annual Report, 1977 (unpublished); University of Groningen Annual Report, 1979 (unpublished).

[19]R. A. Ost, N. E. Sanderson, J. M. A. England, J. P. Nelson, B. Fulton, and G. C. Morrison, University of Birmingham Annual Report, 1975 (unpublished).

[20]Tsan Ung Chan, M. Agard, J. F. Bruandet, and C. Morand, Phys. Rev. C 19, 244 (1979).

[21]C. C. Chang, M. T. Collons, R. W. Koontz, J. R. Wu, and H. D. Holmgren, Bull. Am. Phys. Soc. 24, 631 (1979).

[22]R. A. Lindgren, M. A. Plum, R. S. Hicks, B. Pasker, G. A. Peterson, X. K. Moruyana, and C. F. Williamson, Proceedings of the International Conference on Nuclear Physics, Berkeley, California, 1980, Vol. 1 Abstracts, Lawrence Berkeley Laboratory Report LBL-11118, 1980, p. 79.